Acta Cryst. (1996). B52, 580–585

Structure of $Ce_2Pt_6Ga_{15}$: Interplanar Disorder from the Ce_2Ga_3 Layers

G. H. KWEI,[a] A. C. LAWSON,[b] A. C. LARSON,[b] B. MOROSIN,[c] E. M. LARSON[d] AND P. C. CANFIELD[e]

[a]*Lawrence Livermore National Laboratory, Livermore, CA 94550, USA,* [b]*Los Alamos National Laboratory, Los Alamos, NM 87545, USA,* [c]*Sandia National Laboratory, Albuquerque, NM 87123, USA,* [d]*Grand Canyon University, Phoenix, AZ 85017, USA, and* [e]*Ames Laboratory and Department of Physics and Astronomy, Iowa State University, Ames, IA 50011, USA. E-mail: kwei2@llnl.gov*

(Received 15 December 1995; accepted 15 January 1996)

Abstract

The structure of the heavy fermion compound $Ce_2Pt_6Ga_{15}$ has been determined from neutron powder and X-ray/neutron single-crystal diffraction. Examination of symmetry equivalence among the single-crystal data, as well as the good fit of the powder data to the final structural arrangement, with all the atoms on symmetry sites, suggests that the correct space group is $P6_3/mmc$. The structure is unusual in that Ce layers have 1/3 of the Ce atoms replaced by groups of three Ga atoms; distances between atoms in these planes suggest this substitution must occur in a concerted fashion. The refined occupancies lead to a stoichiometry near $Ce_2Pt_6Ga_{15}$, consistent with such an arrangement. In addition, single-crystal neutron diffraction data show columns of weak diffuse scattering along the <001> axes, suggesting disorder arising from a lack of registration of successive Ce_2Ga_3 layers (lying half a cell length or 8.27 Å apart along **z**) and a $3 \times 3 \times 1$ supercell. This disorder is very likely responsible for the low resistance ratio of approximately unity measured for single crystal samples.

1. Introduction

The newly discovered class of heavy fermion compounds $RE_2Pt_6Ga_{15}$ (RE = rare earth) readily crystallizes into large well formed hexagonal prism-shaped crystals. This family of compounds exhibits extremely interesting, but still poorly understood, magnetic and transport properties (Lacerda *et al.*, 1992). The poor resistance ratio [R(300 K)/R(2 K)] of the order unity suggests that the crystals may be disordered. Clearly, a better understanding of the properties of these materials requires a better knowledge of the structure and an understanding of the nature of the possible disorder. An earlier single-crystal X-ray determination of the structure of $Ce_2Pt_6Ga_{15}$, referred to as $Ce_{2-x}Pt_4Ga_{8+y}$ in earlier work (Lacerda *et al.*, 1992), suggested that the structure conformed to a primitive-hexagonal space group, but a Fourier map suggested a Ga site too close to the Ce site (Burns & Barnhart, 1992). The absorption corrections in these X-ray data were very large and, as a result, the correctness of the structure remained unconfirmed. In the subsequent article (Lacerda *et al.*, 1992) we presented the results of preliminary structural refinements in the space group $P\bar{3}1c$ using powder neutron diffraction data that suggested the earlier structure to be basically correct, but with both Ce and Ga sites partially occupied, most likely with vacancies correlated to avoid close Ce and Ga encounters. One of the issues raised in this work was the degree of correlation of the vacancies and if a larger ordered cell would provide a better description. In this article we report new X-ray and neutron single-crystal data sets to examine whether supercells may better describe the Ce and Ga vacancy ordering and carry out further analysis of the neutron powder data in the space group $P6_3/mmc$. In addition to confirming this choice of space group, the new single-crystal data analysis, together with the neutron powder data refinements, confirm the identity of the Ce and Ga atoms in the Ce_2Ga_3 layers, because of the different relative scattering strengths for the constituent atoms. Additionally, the single-crystal neutron diffraction data show columns of diffuse scattering along the <001> axes and suggest a model for the disorder. Thus, the sum total of the diffraction data provides a detailed model for the structure of $Ce_2Pt_6Ga_{15}$ and elucidates the nature of the disorder. X-ray absorption fine structure (XAFS) data, collected to corroborate the initial disorder model, are also described.

2. Experimental

2.1. *Sample preparation*

Large hexagonal cross section crystals (20 mm^3) of $Ce_2Pt_6Ga_{15}$ (shown in Fig. 1) were grown from a Ga flux using 99.9% purity Pt, 99.99% purity Ga and Ames Laboratory Ce (99.99%+ purity). SEM (scanning electron microscopy) analysis of three points on a sample single crystal gave average values of 9.3, 22.0 and 68.7% for the Ce, Pt and Ga content, in approximate agreement with the stoichiometries found later in the neutron powder and the X-ray/neutron single-crystal structure refinements.

2.2. *Data collection*

Three different diffraction studies and an XAFS study were carried out for the final structure determination. Neutron powder diffraction data were used to refine the structure of $Ce_2Pt_6Ga_{15}$ in space group $P6_3/mmc$. X-ray single-crystal diffraction experiments verified the correctness of the choice of space group and helped identify the occupants of the Ce and Ga(3) sites. The greater dynamic range of the area detectors in the neutron single-crystal diffraction experiments allowed us to observe the expected diffuse scattering streaks resulting from the disordered structure. Finally, XAFS data was used to check the local environment around the Pt and Ga sites and to search for any unusual bond distances between Ga and its nearest neighbors.

Initially, neutron data were collected at room temperature (297 K) from a 2 g powder sample, ground from single crystals, using the ±150, ±90 and ±60° detector banks of the high-resolution general purpose powder diffractometer (GPPD) at the intense pulsed neutron source (IPNS) at Argonne National Laboratory. Sample data are shown in Fig. 2. In addition, XAFS data were collected in the transmission mode at the Stanford Synchrotron Radiation Laboratory (SSRL) on Beam Line 7-3, using a Si(220) double crystal monochromator. These consisted of scans of the Ga K, Pt L_{III}, and Ce L_I and L_{III} edges.

The difficulty in understanding the final crystal structure results and some problems with the powder profile fit prompted the collection of a room-temperature neutron single-crystal data set on the single crystal diffractometer (SCD) at the Manuel Lujan Jr Neutron Scattering Center (MLNSC) and a high-quality X-ray data set at Sandia National Laboratory using crystals from the same batch as used earlier. The crystal used on SCD was a hexagonal prism 1 mm in cross section and 1.5 mm long. There were 11 histograms of data collected using neutron wavelengths λ = 0.63–7.56 Å. Each histogram measured *ca* 125 reflections. Thus, a total of 1534 reflections were measured. The 1416 reflections with $\sigma_I/I > 1.0$ were used in the refinement. The X-ray single-crystal intensity data were collected using Mo $K\alpha$ radiation from a small hexagonal prism 0.034 mm in cross section and 0.45 mm long. There were 728 different *hkl*'s measured on a commercial Nicolet P3 system, some several times during the course of this study.

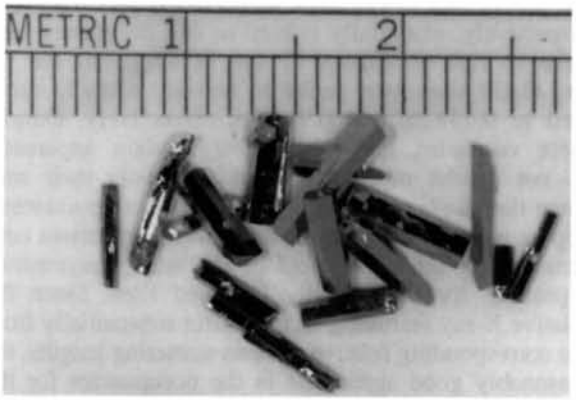

Fig. 1. Photo of a typical crystal of $Ce_2Pt_6Ga_{15}$. The small divisions in the scale at the top measure in mm.

2.3. *Structure refinements and analysis*

Various structural models were examined by Rietveld refinement (Larson & Von Dreele, 1987) using the neutron powder diffraction data. The Bragg peaks were well indexed on the hexagonal basis and we found that the space group $P6_3/mmc$ gave the best fit. In the final structural refinements, sample absorption, powder extinction and the anisotropic strain terms in the profile coefficients, in addition to the usual lattice parameters, atomic positions and either isotropic or anisotropic displacement parameters, were refined. The backgrounds were modeled with a four-term polynomial in Q^{2n}/n with refineable coefficients. The latest recommended values of neutron scattering lengths of 0.484, 0.950 and 0.729×10^{-12} cm for Ce, Pt and Ga, respectively, were used (Sears, 1992). Structural parameters obtained from the Rietveld refinement for the anisotropic displacement parameter model are given in Table 1.* There is little difference between the isotropic and anisotropic refinements, with the value of χ^2_{red} only improving from 4.259 to 4.196 on going to the anisotropic model. Even

* Primary diffraction data have been deposited with the IUCr (Reference: VS0127). Copies may be obtained through The Managing Editor, International Union of Crystallography, 5 Abbey Square, Chester CH1 2HU, England.

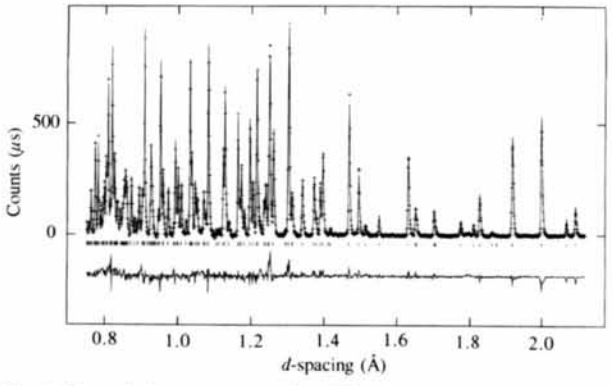

Fig. 2. Part of the neutron powder diffraction data for $Ce_2Pt_6Ga_{15}$ at 297 K. The points shown by plus (+) marks represent data collected on the summed 150° detector banks of the GPPD. The continuous line through the data is the calculated profile from Rietveld refinement with anisotropic displacement parameters. The tick marks below the data indicate the positions of the allowed reflections for $Ce_2Pt_6Ga_{15}$ in the $P6_3/mmc$ space group. The lower curve represents the difference between the observed and calculated profiles.

Table 1. *Structural parameters for $Ce_2Pt_6Ga_{15}$ (space group $P6_3/mmc$) at 297 K from Rietveld refinement with anisotropic displacement parameters using neutron powder diffraction data* and least-squares refinement using Mo Kα X-ray† and neutron single-crystal diffraction data*

	Neutron powder	X-ray single crystal	Neutron single crystal
Lattice parameters (Å):			
a	4.32674 (21)	4.335 (10)	4.3259 (5)
c	16.5369 (8)	16.564 (7)	16.5216 (26)
Cell volume (Å^3)			
V	268.11 (3)	269.7 (2)	267.76 (1)
Occupancy, lattice positions and displacement parameters			
Ce 2*c* (1/3,2/3,1/4)			
f	0.639 (6)	0.690 (8)	0.632 (12)
$U_{11} \equiv U_{22} \equiv 2U_{12}$	5.5 (7)	5.1 (8)	3.6 (9)
U_{33}	8.1 (13)	11.6 (10)	−0.3 (11)
U_{eq}	5.5 (7)	7.2 (8)	1.7 (9)
Pt 4*f* (2/3,1/3,*z*)			
z	0.39188 (4)	0.39214 (4)	0.39203 (4)
$U_{11} \equiv U_{22} \equiv 2U_{12}$	9.22 (24)	7.4 (9)	5.08 (21)
U_{33}	7.0 (4)	14.0 (4)	3.72 (32)
U_{eq}	6.9 (3)	9.6 (9)	3.8 (2)
Ga(1) 4*f* (2/3,1/3,*z*)			
f	0.995 (4)	1.0	1.0
z	0.54609 (5)	0.54631 (12)	0.54604 (6)
$U_{11} \equiv U_{22} \equiv 2U_{12}$	11.24 (29)	9.6 (5)	7.71 (25)
U_{33}	8.1 (5)	13.7 (4)	3.6 (4)
U_{eq}	8.3 (3)	10.9 (5)	5.1 (3)
Ga(2) 4*e* (0,0,*z*)			
f	0.984 (4)	1.0	1.0
z	0.36413 (5)	0.363124 (10)	0.36457 (6)
$U_{11} \equiv U_{22} \equiv 2U_{12}$	10.3 (3)	5.6 (6)	6.29 (25)
U_{33}	13.8 (5)	15.6 (10)	10.3 (5)
U_{eq}	9.7 (3)	8.9 (6)	6.6 (3)
Ga(3) 6*h* (x,$-x$,1/4)			
f	0.314 (3)	0.305 (5)	0.311 (5)
$x \equiv -y$	0.53429 (26)	0.5304 (5)	0.53325 (32)
$U_{11} \equiv U_{22}$	14.8 (10)	-	8.2 (9)
U_{33}	2.2 (9)	-	2.6 (10)
U_{12}	9.1(9)	-	6.0 (9)
U_{eq}/U_{iso}	7.6 (10)	5.2 (10)	4.4 (10)
Chemical formula	$Ce_{1.92}Pt_6Ga_{14.82}$	$Ce_{2.07}Pt_6Ga_{14.75}$	$Ce_{1.89}Pt_6Ga_{14.81}$
R_{wp}/R_{exp} (%)	7.97/5.35	3.12/2.86	6.4/7.2
χ^2_{red}	4.196	0.469	13.64

* Numbers in parentheses following the refined parameters represent one standard deviation in the last digit(s). Units for the displacement parameters are 1000 Å^2. $U_{13} \equiv U_{23} \equiv 0$ by symmetry. U_{eq} is calculated from the anisotropic displacement parameters using the definition $U_{eq} = 1/3\mathrm{Tr}\mathbf{U}$. Ga stoichiometry is calculated assuming Ga(1) and Ga(2) sites are fully occupied. † The X-ray structure analysis assumed Ga(1) and Ga(2) were fully occupied and employed only an isotropic displacement parameter for Ga(3).

with the anisotropic model, the thermal ellipsoids for Ce, Pt, Ga(1) and Ga(2) are almost spherical; however, those for Ga(3) are compressed along the *c*-axis to give pancake-shaped ellipsoids.

All the single crystal data for the Laue group $\bar{3}m2$ in both the neutron and X-ray data cases were measured. Averaging the X-ray data over the Laue group 6/*mmm* equivalents gave R_{int} = 1.64%, indicating that to be the true symmetry. The absorption-corrected multiple observations were averaged to yield 154 independent *hkl* values for the X-ray data. Similar symmetry-related averaging was not carried out on the neutron single-crystal data. The results are not reliable until after the final structural refinements when the extinction correction is known and can be applied to the observations. The absence of 00*l*, $l = 2n + 1$, and *hhl*, $l = 2n + 1$, indicates the space group to be $P6_3/mmc$ or $P6_3mc$.

A structural model was developed for the X-ray single-crystal data independent of the previous work using Patterson and Fourier techniques, together with least-squares refinement of the positional parameters. The *SHELXS*86 (Sheldrick, 1985) software system was employed for these calculations. This leads to essentially the same structural model with small parameter differences from those determined by the neutron powder Rietveld refinement.

The lattice constants, positional and displacement parameters, and the site occupancies from the structural refinements from three different diffraction studies are given in Table 1. The refined values for the lattice constants, positional parameters and the site occupancies generally agree quite well, although some differences, such as differences in the lattice parameters and the Ce site occupancy between the neutron and X-ray studies, do exist. It is not clear whether these differences arise from the different measurement techniques or from sample variation. The agreement for the displacement parameters is not nearly as good, but these variables are very sensitive to the incident spectrum used in the TOF experiments and to the absorption and extinction models used in all experiments. The interatomic distances calculated from the lattice parameters and the atomic positions are given in Table 2. Here again, the agreement is generally good; however, the small differences in such parameters for Ga(3) in Table 1 lead to some significant differences in the atomic distances involving Ga(3).

For the neutron powder structures, the occupancy of the Ga(1) and Ga(2) sites at 0.995 (4) and 0.984 (4), respectively, essentially refined to full occupancy (relative to full occupancy of the Pt site), but the Ce and Ga(3) sites were found to be only partially occupied at 0.639 (6) and 0.314 (3), respectively. Despite these vacancies, the Ce and Ga(3) atoms apparently do not exhibit much static disorder about their sites since the in-plane anisotropic displacement parameters appear normal. The X-ray data provides important confirmation of the correctness of the atom assignments, especially for the partially occupied sites. Since the relative X-ray scattering factors differ substantially from the corresponding relative neutron scattering lengths, the reasonably good agreement in the occupancies for the partially vacant Ce and Ga(3) sites between the X-ray refinements [0.690 (8) and 0.305 (5), respectively] and

the neutron powder refinements [0.639 (6) and 0.314 (3), respectively] confirm our earlier assignment.

The partial occupancy of approximately 2/3 and 1/3 for the Ce and Ga(3) sites is intriguing and suggests that the unit cell found might be a subcell of the true cell and that a larger cell with ordered vacancies may exist. However, the failure of numerous trial-and-error attempts to fit larger cells, involving doubling or tripling of the cell along the different axes, to the neutron powder diffraction data suggested that the original smaller cell was in fact the correct choice.

Examination of the neutron single-crystal data revealed columns of diffuse scattering along [001] at $h \pm 1/3$, $k \pm 2/3$. The intensity of these streaks was of the order 10^{-4} of the Bragg reflections. Fig. 3 shows the $h,h-2,l$ lattice net centered on the 310 reflection. The $h,h-2,0$ vector is horizontal increasing to the right and $00l$ points upward in the plot. The columns of discrete peaks are the $20l$, $31l$ and $42l$ lattice rows. There are prominent streaks from diffuse scattering along the 8/3,2/3,*l* and 10/3,4/3,*l* lattice rows, and there are somewhat weaker diffuse streaks along the 7/3,1/3,l and 11/3,5/3,l lattice rows. Further examination of the neutron single-crystal data did not show the presence of any superlattice reflections, ruling that out as the cause of the problem.

An examination of the Ce–Ga(3) planes shows that one can define a filled two-dimensional net in a concerted arrangement which removes short (~1.5 and 1.75 Å) separations. This net has symmetry $p3m1$ and requires a cell which is tripled in x and y relative to the observed unit cell. Since these layers are 8.27 Å apart, it is not surprising that they would not register with each other to triple the a axis, but rather are randomly positioned relative to the remainder of the structure between the Ce—Ga(3) layers. This layer has the composition Ce_2Ga_3 and is illustrated in Fig. 4. The diffuse streaks in the neutron single-crystal data arise from this failure of the various Ce_2Ga_3 layers to align with one another in a coherent manner. This ordered two-dimensional structure, disordered along the c-axis, gives rise to the partial occupancy of the Ce and Ga(3) sites.

The Pt and Ga X-ray absorption data were adequate in providing both XANES and XAFS portions of the spectra. Backgrounds were subtracted using a cubic-spline routine. The absolute energy was established for each spectrum by calibration to the edges of standard materials (for example Pt metal for the Pt edge). Details of the data reduction procedures are given elsewhere (Lytle, Via & Sinfelt, 1980). Phase information for the Ga radial distribution function was calculated using FEFF5 (Mustre de Leon, Rehr, Zabinsky & Albers, 1991; Rehr, Mustre de Leon, Zabinsky & Albers, 1991) and the published structural parameters for Ga_3Pt_5 (Bhan & Schubert, 1960). A comparison was made between the experimental radial distribution functions obtained from the Pt L_{III} edge data for $Ce_2Pt_6Ga_{15}$ and the calculated spectrum using FEFF5 for the structure given in Table 1. This agreement supports the nearest-neighbor environment around the Pt given by the structural parameters obtained in the diffraction experiments. The radial distribution function about the Ga sites can be obtained from

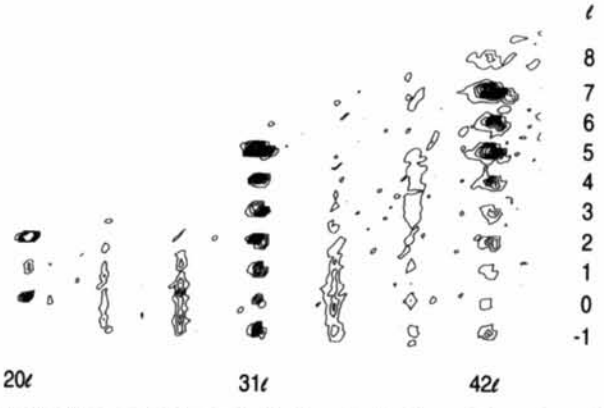

Fig. 3. Diffuse scattering in $Ce_2Pt_6Ga_{15}$. A slice through the reciprocal space coverage of one histogram. Plotted are the $20l$, $31l$ and $42l$ lattice rows showing the diffuse scattering along 7/3,1/3,*l*; 8/3,2/3,*l*; 10/3,4/3,*l*; 11/3,5/3,*l*. The upper and lower edges of the plot field are limited by the edges of the detector. Contours are at arbitrary values of 1, 2, 4, 8 *etc.*

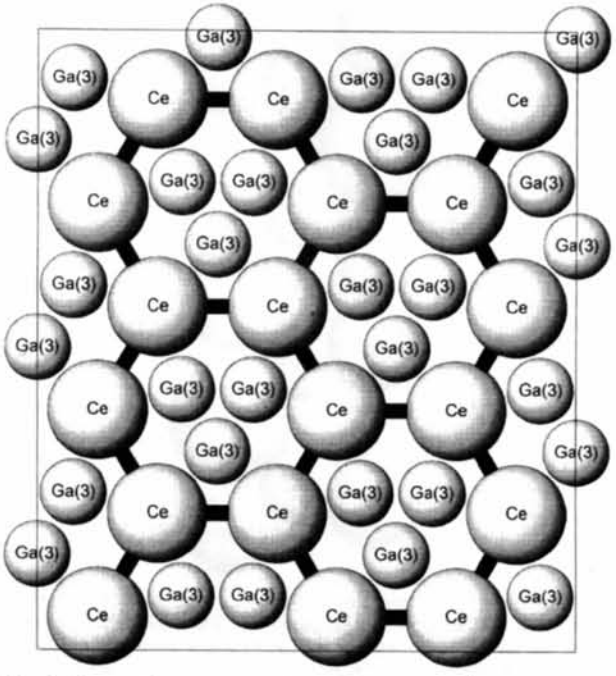

Fig. 4. Proposed arrangement for a 22.5 × 19.5 Å section of the Ce–Ga(3) net. Three smaller Ga(3) atoms about the threefold axes occupy the space of the absent Ce. This net contains two Ce for every three Ga, as determined by the structure refinements. The concerted arrangement requires a tripled cell in x and y relative to the observed unit cell.

the Ga *K* edge data and is shown in Fig. 5. The distances in the local Ga coordination environments (for all Ga sites) are all greater than ~2.5 Å, which also agrees with the model from diffraction experiments. As shown in Table 2, the latter give Ga—Ga distances ranging from 2.61 to 2.93 Å, Ga—Pt distances from 2.54 to 2.70 Å and Ga—Ce distances from 3.13 to 3.37 Å, with the short Ce—Ga(3) (1.51 Å) and Ga(3)—Ga(3) (1.72 Å) distances absent because of the concerted structure in the Ce_2Ga_3 nets.

3. Discussion

The structure can be described as two-dimensional nets of Ce_2Ga_3 atoms perpendicular to the *c* axis that are separated by Pt—Ga slabs. The Ce—Ce separation within the nets is 4.33 Å and the distance between the nets is 8.27 Å. These nets consist of a concerted arrangement of Ce and Ga(3), as shown in Fig. 4. The relative position of one of these nets with respect to other Ce_2Ga_3 nets is not ordered.

As shown in Fig. 6, the structural packing may possibly be best visualized as a rather distorted close-packed arrangement of spheres with a 14 layer repeat, *ABCDCBAABCECBA*..., in which the *A*, *B* and *C* layers, corresponding to the Ga(1), Pt and Ga(2) layers, respectively, are the usual layers defining cubic close-pack spheres and in which the *D* and *E* layers contain the concerted 3 × 3 Ce_2Ga_3 nets [with Ga(3) atoms]. The *D* and *E* layers would correspond to *A* and *B* layers, respectively, if only Ce were present. In Fig. 4 the actual metal types label the various spheres. The symmetry-related *D* and *E* layers each really contain only 2/3 Ce and 1 Ga(3) in each layer within the hexagonal cell, as shown in the extended arrangement shown in Fig. 4. The principal disorder in the structure is interplanar, arising from the random positions of the Ga(3) clusters in the nets at subsequent *z*-levels of the structure. Because of the interplanar disorder, there is no direct diffraction evidence for the detailed structure of the net, the only evidence of the disorder is

Table 2. *Nearest-neighbor atom distances (Å) in $Ce_2Pt_6Ga_{15}$ at 297 K**

Atom pair	Multiplicity	Neutron powder	X-ray single crystal	Neutron single crystal
Ce—Ce	3	4.32674 (21)	4.335 (10)	4.3259 (5)
Ce—Pt	6	3.4271 (4)	3.437 (1)	3.4270 (6)
Ce—Ga(1)	2	3.3721 (8)	3.374 (1)	3.3698 (11)
Ce—Ga(2)	6	3.1309 (6)	3.128 (1)	3.1338 (7)
Ce—Ga(3)	3†	1.5060 (20)	1.480 (1)	1.4979 (24)
	6	3.1149 (14)	3.142 (1)	3.1199 (18)
Pt—Ga(1)	1	2.5501 (10)	2.554 (1)	2.5443 (13)
	3	2.7005 (4)	2.703 (1)	2.6990 (5)
Pt—Ga(2)	3	2.53984 (20)	2.549 (1)	2.5385 (4)
Pt—Ga(3)	3	2.5474 (9)	2.567 (1)	2.5507 (12)
Ga(1)—Ga(1)	3	2.9264 (8)	2.936 (1)	2.9243 (10)
Ga(1)—Ga(2)	3	2.9059 (6)	2.917 (1)	2.9016 (8)
Ga(2)—Ga(3)	6	2.8825 (6)	2.876 (1)	2.8851 (8)
Ga(3)—Ga(3)	2†	1.7183 (34)	1.772 (1)	1.732 (4)
	2	2.6084 (34)	2.564 (1)	2.594 (4)

* Numbers in parentheses following refined parameters represent one standard deviation in the last digit(s). † These distances exist in a completely disordered model, not in the present case with its concerted arrangement (see text).

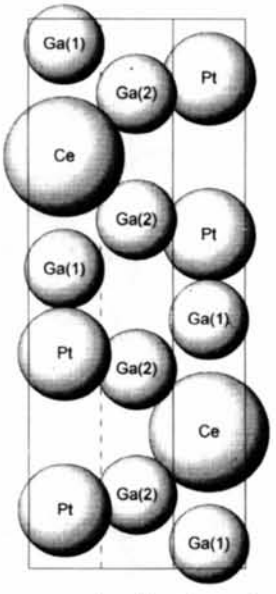

Fig. 5. Scheme of the structural packing in a unit cell of $Ce_2Pt_6Ga_{15}$ showing the close-packing arrangement. The various atoms show the 14 layer repeat, *ABCDCBAABCECBA*..., from the top down and in which the Ga(1), Pt and Ga(2) atoms, corresponding to the *A*, *B* and *C* layers, respectively, are the usual layers defining cubic close-packed spheres, and in which the concerted 3 × 3 Ce_2Ga_3 nets [with Ga(3) atoms] correspond to the *D* and *E* layers. The *D* and *E* mirror planes are shown in detail in Fig. 4. The differing sizes of the metal atoms (metallic radii are 1.72, 1.38 and 1.22 Å for Ce, Pt and Ga, respectively) distort the ideal packing along the *c* axis.

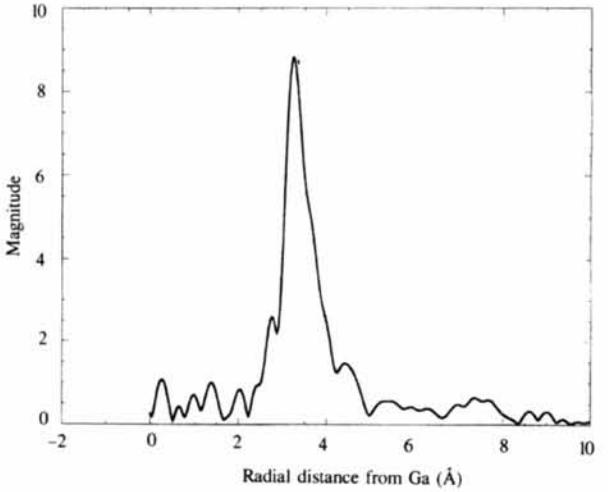

Fig. 6. Phase-corrected radial distribution of atoms about Ga from Ga *K* edge XAFS.

the diffuse scattering seen in the single-crystal neutron data. The Ce site occupancy is 0.639 (6) from powder neutron data, 0.690 (8) from single-crystal X-ray data and 0.632 (12) from single-crystal neutron data, with only the X-ray value greater than the expected value of 2/3. The Ga(3) site occupancy is estimated at 0.314 (3), 0.305 (5) and 0.311 (5), respectively, all a little lower than the expected value of 1/3. The deviation of the observed occupancies from the ideal values of 2/3 and 1/3, respectively, may indicate some intraplanar disorder; this would involve the orientational disorder of the Ga(3) clusters, that cannot be accommodated without some intraplanar vacancies.

An attempt was made to use a model based on a disordered supercell with the *ortho*-hexagonal symmetry space group *Cmcm*. This cell can be obtained from the $P6_3/mmc$ cell using the transformation matrix (3,0,0;1,2,0;0,0,1) and has lattice constants a = 12.980, b = 7.493 and c = 16.537 Å. However, we could not obtain stable refinements for the lattice constants or the atomic parameters. Presumably, these refinements failed to converge because there is little ordering of the Ce_2Ga_3 layers with respect to each other. The question of ordering is complicated by the fact that the threefold axis of the net does not coincide with the 6_3-axis of the main structure, but rather with one of the 3-axes at 1/3,2/3,z. The disorder results from competition between two-dimensional ordering in the net and three-dimensional ordering in the Pt–Ga blocks.

We do not know how the extent of disorder in the registration of the RE_2Ga_3 nets depends on the crystal growth and whether or not long anneals might produce more ordered crystals. We suspect that the large 8.27 Å layer separations result in too low a driving force for ordering at temperatures where the constituents are still mobile. It would be interesting to see if the resistance ratio of such an annealed sample is different from unity and if it is, how much the diffuse scattering is diminished. However, initial anneals of up to 100 Å at 773 K have shown no change in the resistance ratio.

Earlier rough estimates of the rare-earth concentration from susceptibility data for $RE_2Pt_6Ga_{15}$ compounds show that it is reasonably constant in these materials, ranging from 1.91 for RE = Nd to 2.21 for RE = Ce (Lacerda *et al.*, 1992). The site occupancy for Ce from our studies is consistent with these values, giving more accurate values of the overall Ce concentration that range from 1.89 to 2.07. This suggests that the structures of the $RE_2Pt_6Ga_{15}$ compounds are similar with similar RE_2Ga_3 nets. The structures of these compounds, with the large separation between the nets, suggest that they should provide a unique opportunity for further studies of the effects of doping of impurities into almost isolated two-dimensional rare-earth layers.

We thank Paula Newcomer of Sandia National Laboratory for the SEM analysis of the sample composition and Joyce Roberts of the MLNSC at Los Alamos, Jim Richardson of the Argonne National Laboratory and the scientist responsible for the GPPD for their help in carrying out the neutron powder diffraction experiments. The neutron powder diffraction data were collected on the GPPD at the Intense Pulsed Neutron Source at Argonne National Laboratory and the neutron single-crystal data were collected on the single crystal diffractometer (SCD) at the Manuel Lujan Jr Neutron Scattering Center at the Los Alamos National Laboratory. Both are funded as national user facilities by the Division of Material Sciences, Office of Basic Energy Sciences (OBES) of the United States Department of Energy (DOE). The synchrotron data was collected at the Stanford Synchrotron Radiation Laboratory (SSRL), which is funded by the Division of Chemical Sciences, DOE/OBES and by the National Institutes of Health, Division of Research Resources. Figures 4 and 5 were prepared using the program *Atoms*, written by Eric Dowty of Shape Software. All work was performed under the auspices of DOE: the work at Lawrence Livermore National Laboratory under contract W-7405-ENG-48, the work at Los Alamos National Laboratory under contract W-7405-ENG-36, the work at Sandia National Laboratory under contract WE-AC04-76DP00789 and the work at Ames Laboratory under contract W-7405-ENG-82.

References

Bhan, S. & Schubert, K. (1960). *Z. Metallkd.* **51**, 327–339.

Burns, C. & Barnhart, D. (1992). Unpublished results.

Lacerda, A., Canfield, P. C., Beyermann, W. P., Hundley, M. F., Thompson, J. D., Sparn, G., Fisk, Z., Burns, C., Barnhart, D., Lawson, A. C., Kwei, G. H. & Goldstone, J. A. (1992). *J. Alloys Compd.* **181**, 191–196.

Larson, A. C. & Von Dreele, R. B. (1987). Report LA-UR-86-748. Los Alamos National Laboratory, New Mexico, USA.

Lytle, F. W., Via, G. H. & Sinfelt, J. H. (1980). *Synchrotron Radiation Research*, edited by H. Winick & S. Doniach, pp. 401–424. New York: Plenum Press.

Mustre de Leon, J., Rehr, J. J., Zabinsky, S. I. & Albers, R. C. (1991). *Phys. Rev. B*, **44**, 4146–4156.

Rehr, J. J., Mustre de Leon, J., Zabinsky, S. I. & Albers, R. C. (1991). *J. Am. Chem. Soc.* **113**, 5135–5140.

Sears, V. F. (1992), *Neutron News*, **3**, 26–37.

Sheldrick, G. M. (1985). *SHELXS86. Program for the Solution of Crystal Structures*. University of Göttingen, Germany.